



Design of delay timers based on estimated probability mass functions of alarm durations[☆]

Jiandong Wang^{a,*}, Zhen Wang^a, Xuan Zhou^a, Fan Yang^b

^a Shandong University of Science and Technology, Qingdao, Shandong Province, China

^b Department of Automation, Tsinghua University, Beijing, China



ARTICLE INFO

Article history:

Received 30 July 2021

Received in revised form 14 November 2021

Accepted 2 January 2022

Available online 11 January 2022

Keywords:

Alarm systems

Delay timers

False alarms

Bayesian estimation

Alarm durations

ABSTRACT

Delay timers are widely used in practice to remove nuisance alarms. This paper proposes a method to design delay timers based on probability mass functions (PMFs) of alarm durations. The main rationale is that all nuisance alarms with alarm durations less than m samples are removed by a m -sample delay timer. The proposed method is composed of three steps. First, distribution change points of alarm durations are detected to separate consecutive samples of alarm durations into segments. Second, a reliable PMF estimate of alarm durations is obtained via the Bayesian estimation for each segment. Third, an optimal value of m is designed based on the estimated PMFs as the smallest one to make a designing index, being formulated as the percentage of false alarm occurrences to be unremoved, less than an upper bound. Contemporary methods are confined to analog process variables, which are usually assumed to be independently and identically distributed (IID) and whose probability density functions are exploited to design delay timers. In contrast, the proposed method does not require the IID assumption, and is equally applicable to both analog and digital process variables. Numerical and industrial examples are provided to support the proposed method.

© 2022 Elsevier Ltd. All rights reserved.

1. Introduction

Alarm systems play an important role for operational safety and efficiency of industrial plants [1,2]. When abnormalities occur, process variables are deviated from normal operating ranges so that alarms are announced automatically to notify industrial plant operators for taking prompt reactions. The performance of alarm systems has received persisting attentions from both industrial and academic communities [3,4].

Nuisance alarms are often observed in practice, distracting industrial plant operators from noticing true alarms [5,6], and need to be removed before advanced processing of alarm messages [7–9]. Many advanced alarm process methods rely heavily on the information of true alarms, such as alarm pattern mining [10], alarm root cause diagnosis [11], alarm prediction [12], and risk/event-based approaches for alarm management [13–16]. A common prerequisite therein is that most of the occurring alarms are caused by actual abnormal conditions, while nuisance alarms due to the presence of noises and disturbances usually

play a detrimental role to these advanced alarm processing methods. For instance, it is meaningless to trigger the root cause analysis for a nuisance alarm.

The m -sample delay timer is widely used in industrial alarm systems to remove nuisance alarms, by raising (clearing) alarms if and only if m consecutive samples are in the alarm (non-alarm) state [1,2]. Hollifield and Habibi [17] recommended 15 s, 30 s and 60 s as default values of delay timers respectively for flow, pressure and temperature process variables. Adnan et al. [18], Naghossi et al. [19] calculated three performance indices of delay timers for Markov processes, namely, false alarm rates (FAR), missing alarm rates (MAR), and expected detection delays (EDD) to announce abnormality occurrences. Xu et al. [20] designed delay timers by minimizing a sum of normalized FAR, MAR and EDD based on estimated probability density functions of process variables in normal and abnormal conditions. Adnan et al. [21] derived analytic expressions of the FAR, MAR and EDD for generalized delay timers, where m_1 out of m consecutive samples in the alarm (non-alarm) state are required to raise (clear) an alarm. Wang and Chen [22] adjusted parameters of delay timers in an online manner for chattering and repeating alarms, according to statistics of oscillation periods or alarm intervals and durations. Afzal et al. [23] developed expressions of the FAR, MAR and EDD of multimode delay timers for processes under multiple operating modes with same or different alarm thresholds. Zeng et al. [24] evaluated the performance

[☆] This research was supported by the National Natural Science Foundation of China under grant No. 61433001.

* Corresponding author.

E-mail addresses: jiantong@sdust.edu.cn (J. Wang), wzz4585@163.com (Z. Wang), xuan_zhou178@163.com (X. Zhou), yangfan@tsinghua.edu.cn (F. Yang).

of generalized delay timers including m_1 out of m samples off-delay timers, n_1 out of n samples on-delay timers and their combinations. Tulsyan et al. [25] exploited particle filters for designing delay timers for nonlinear process variables that could be represented by a class of stochastic models. Afzal and Chen [26] analyzed performance indices of time-deadbands (as cousins of delay timers) that wait for certain time periods before raising or clearing alarms. Su et al. [27] advocated multi-setpoint delay timers, raising (clearing) alarms for m consecutive samples or one single sample depending on the deviation levels of process variables away from normal ranges. Taheri-Kalani et al. [28] introduced a penalty term to generalized delay timers as an extra degree of freedom in m_1 out of m consecutive samples. Kaced et al. [29] extended generalized delay timers by using different alarm thresholds respectively for process variables in normal and abnormal conditions. Wang et al. [30] formulated an index to determine whether a delay timer or an alarm deadband is suitable for removing nuisance alarms.

The main contribution of this paper is to propose an alarm-duration-based method for designing the m -sample delay timer. The method is based on a close relation between the delay factor m and the alarm duration that is the number of samples in the alarm state. All nuisance alarms with alarm durations less than m samples are removed by a m -sample delay timer. By assuming the availability of historical data samples in the normal condition, the proposed method is composed of three steps. First, the alarm durations are separated into several segments based on a distribution change detection approach. Second, a reliable estimation of the probability mass function (PMF) for each alarm durations segment is obtained by exploiting the Bayesian estimation approach. Third, the proper delay factor for each alarm durations segment is designed from the estimated PMF, as the smallest one to satisfy an upper bound requirement on the percentage of false alarm occurrences to be unremoved by a delay timer. An optimal value of m is obtained as the maximum one of these delay factors.

The main feature of the proposed method is the exploitation of probability distributions of *alarm durations*, whereas most of contemporary methods are based on probability distributions of *process variables*. The main feature leads to two advantages: (i) The proposed method is applicable to both analog and digital process variables, while most of contemporary methods are confined to analog ones. For instance, 2226 alarm variables are configured for 208 analog and 2018 digital process variables in a 300MW thermal power generation unit [31]. Hence, it is practically important to have a method equally applicable to both types of process variables. (ii) Contemporary methods require an assumption that process variables are independently and identically distributed (IID), to reach analytic relationships between performance indices and delay timer parameters. For a non-IID process variable, joint probability distributions of consecutive samples of an analog process variable are required, and they are quite demanding to estimate, e.g., via particle filters [25]. In contrast, the proposed method is based on alarm durations so that it does not require the IID assumption on process variables.

The rest of this paper is organized as follows. Section 2 formulates the problem to be solved. Section 3 presents the main idea and detailed steps of the proposed method. Section 4 provides numerical and industrial examples as illustrations. The paper ends with a conclusion at Section 5.

2. Problem formulation

A common way of generating an alarm variable x_a from a process variable x is to set the value of x_a to '1'('0') if x is larger

(less) than a high alarm threshold x_{th} for the alarm (non-alarm) state, i.e.,

$$x_a(t) = \begin{cases} 1, & \text{if } x(t) \geq x_{th} \\ 0, & \text{if } x(t) < x_{th} \end{cases}. \quad (1)$$

Here t is the sampling index being associated with a sampling period h (e.g., $h = 0.2$ sec). Eq. (1) is readily adapted to a low alarm threshold if necessary. When x is in the normal operating condition, some data samples of $\{x_a(t)\}_{t=1}^N$ may run into the alarm state due to the presence of noises and disturbances. As a result, false alarms occur. As a performance index, the false alarm rate (FAR) is the percentage of data samples in the alarm state when x is in the normal condition,

$$f(x_a) = \frac{\sum_{t=1}^N x_a(t)}{N}. \quad (2)$$

If x is in the abnormal condition, then some data samples of $\{x_a(t)\}_{t=1}^N$ may take the non-alarm state, so that missing alarms appear. As another performance index, the missing alarm rate (MAR) can be defined analogously to the FAR; the corresponding definition is omitted here to save spaces.

Delay timers are widely used in practice to remove false alarms. The m -sample delay timer raises (clears) an alarm if and only if m consecutive samples of x_a are '1's ('0's), i.e.,

$$x_{a,m}(t) = \begin{cases} 1, & \text{if } \sum_{i=t-m+1}^t x_a(i) = m \& x_{a,m}(t-1) = 0, \\ 0, & \text{if } \sum_{i=t-m+1}^t x_a(i) = 0 \& x_{a,m}(t-1) = 1, \\ x_{a,m}(t-1), & \text{otherwise.} \end{cases} \quad (3)$$

It is a well-known fact that a larger value of m removes more false and missing alarms, but results in a larger value of the expected detection delay (EDD) that measures the latency of detecting abnormal conditions. If both historical data samples of x in the normal and abnormal conditions are available, then the delay factor m can be designed based on the FAR, MAR and EDD. However, in our experience, most of process variables are in the normal condition for a majority of time periods, and false alarms are the major concerns to industrial plant operators. Hence, only historical data samples of x in the normal condition are assumed here, i.e., $\{x(t)\}_{t=1}^N$ is given as a historical data set where x is in the normal condition.

Alarm occurrences (alarm clearances) are the events that x_a switches from '0' to '1' (from '1' to '0'). The number of alarm occurrences in $\{x_a(t)\}_{t=1}^N$ is

$$O(\{x_a(t)\}_{t=1}^N) = \sum_{t=1}^N x_{a,o}(t),$$

where $x_{a,o}$ takes the value '1' only at the time instant when an alarm occurs, i.e.,

$$x_{a,o}(t) = \begin{cases} 1, & \text{if } x_a(t-1) = 0 \& x_a(t) = 1 \\ 0, & \text{otherwise} \end{cases}.$$

Delay timers are exploited here to reduce the number of false alarms. Industrial plant operators usually respond to each event of alarm occurrences instead of each data sample belonging to the same alarm occurrence. Hence, a designing index η is formulated here as the percentage of false alarm occurrences in $\{x_a(t)\}_{t=1}^N$ to be left in $\{x_{a,m}(t)\}_{t=1}^N$, i.e.,

$$\eta(m) = \frac{O(\{x_{a,m}(t)\}_{t=1}^N)}{O(\{x_a(t)\}_{t=1}^N)}. \quad (4)$$

Note that $\eta(m)$ is in the range $[0, 1]$. This designing index mainly focuses on the reduction of false alarms after applying the alarm

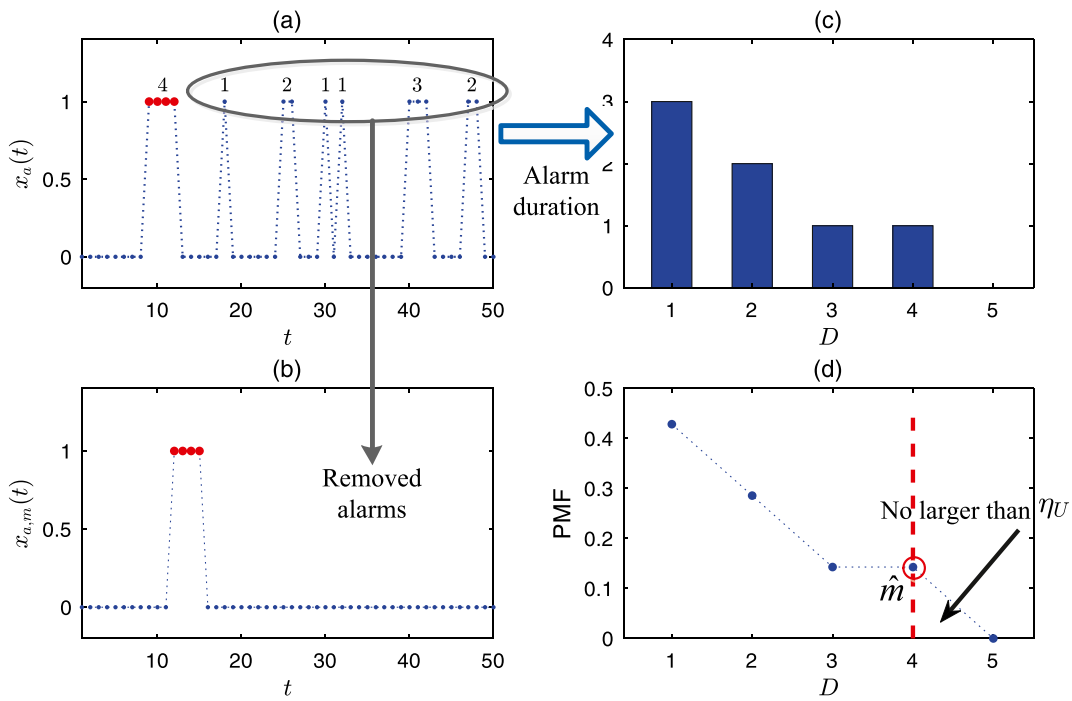


Fig. 1. A schematic illustration of the main idea: (a) Data samples of $x_a(t)$ (blue dash-dotted), (b) $x_{a,m}(t)$ (blue dash-dotted) for $m = 4$, (c) the histogram of alarm durations for $x_a(t)$, (d) the probability mass function (PMF) of D .

delay. In this context, η in Eq. (4) is used to design delay timers, and the FAR in Eq. (2) is taken to evaluate delay timers. Clearly, the FAR will decrease with the decrement of η .

The objective of this paper is to find the smallest value of m in Eq. (3) based on $\{x_a(t)\}_{t=1}^N$, to make $\eta(m)$ in Eq. (4) less than a user-selected upper bound η_U . Note that the MAR and EDD are implicitly considered here, by setting the upper bound η_U and choosing the smallest value of m .

3. The proposed method

This section presents the main idea and detailed steps of the proposed method.

3.1. Main idea

The main idea is illustrated in a schematic figure in Fig. 1. Fig. 1-(a) shows samples of an alarm variable $\{x_a(t)\}_{t=1}^{50}$ in normal conditions. There are 7 nuisance alarms in $x_a(t)$. If the delay factor m is selected as 4, then 6 nuisance alarms in $x_a(t)$ with alarm durations smaller than 4 samples (the blue ones in Fig. 1-(a)) are removed in Fig. 1-(b). An alarm duration D refers to the number of samples of x_a from an alarm occurrence until its clearance. Fig. 1-(c) presents the histogram of D . If D is less than m , then the corresponding alarm occurrence in $x_a(t)$ will disappear in $x_{a,m}(t)$.

Such a close relationship between D and m implies that m can be designed based on the statistics of D . As shown in Fig. 1-(d), given p_D as the probability mass function (PMF) of D , a proper value \hat{m} for m in Eq. (3) is designed as the smallest one satisfying a constraint

$$\sum_{d=\hat{m}}^{+\infty} p_D(d) \leq \eta_U. \quad (5)$$

Here η_U is a user-selected upper bound of $\eta(m)$ in Eq. (4), e.g., $\eta_U = 0.05$.

There are two major technical challenges. First, alarm occurrences and their alarm durations are often mutually independent,

but alarm durations may not be identically distributed due to the changes of operating conditions. Thus, it is necessary to check whether distributions of alarm durations are changing, and to separate samples of alarm durations into segments with different distributions if necessary. Second, a reliable PMF estimate of $p_D(d)$ is critical for designing \hat{m} , so that the designed delay timer is ensured with enough confidence to achieve an expected performance. Hence, it is important to evaluate the PMF estimate reliability in a systematic way. The following two subsections address these technical challenges.

3.2. Delay factor design

As illustrated in the main idea, the proposed method designs m based on alarm durations of x_a , instead of probability density functions (PDFs) of x . The i th alarm duration is

$$D(i) = (t_c(i) - t_o(i) + 1), \quad (6)$$

where $t_o(i)$ and $t_c(i)$ are respectively the sampling indices of the i th alarm occurrence and clearance,

$$x_a(t_o(i) - 1) = 0, \quad x_a(t_c(i) + 1) = 0,$$

$$\sum_{t=t_o(i)}^{t_c(i)} x_a(t) = t_c(i) - t_o(i) + 1, \quad \text{for } t_c(i) \geq t_o(i).$$

D is defined from x_a , so that such a design method is equally applicable to both analog and digital process variables.

The alarm duration D is a discrete random variable with positive integers in the sample space. The PMF p_D can be estimated via a standard PMF estimation algorithm from alarm duration samples $\{D(i)\}_{i=1}^I$ that are obtained from normal historical data samples $\{x_a(t)\}_{t=1}^N$. However, D may not follow the same distribution as the industrial process could experience different operation conditions. A distribution change detection approach is formulated here to determine whether the distribution of D has changed. Next, samples of D are separated into several segments with different distributions based on detected change points. The

approach consists of three sub-steps, where the first sub-step is borrowed from Pettit [32]:

Sub-step 1: For $\{D(i)\}_{i=1}^I$, find one mean change point as follows,

- A test statistic $U_{i,I}$ is calculated as

$$U_{i,I}(t) = \begin{cases} V_{i,I}, & i = 1 \\ U_{i-1,I} + V_{i,I}, & i > 1 \end{cases}, \quad (7)$$

where

$$V_{i,I} = \sum_{j=1}^I \text{sgn}(D(i) - D(j)).$$

Here $\text{sgn}(\cdot)$ is the sign function.

- The index i_{cp} that maximizes $|U_{i,I}|$ is found, and the corresponding P -value is calculated as

$$P = 2 \exp \left(\frac{-6 \max_{1 \leq i < I} (U_{i,I})^2}{I^2 + I^3} \right). \quad (8)$$

- The probability of a type I error α is chosen, e.g., $\alpha = 0.01$. If $P < \alpha$, the distribution of $\{D(i)\}_{i=1}^I$ has changed, and the index i_{cp} is regarded as the change point. Otherwise, the conclusion is that the distribution of $\{D(i)\}_{i=1}^I$ has not changed.

Sub-step 2: Divide $\{D(i)\}_{i=1}^I$ into two segments based on the change point i_{cp} . Go to sub-step 1 for each segment to find their change point, and repeat sub-steps 1 and 2 until no further change points can be found.

Sub-step 3: Separate $\{D(i)\}_{i=1}^I$ into K segments as $\{D(i)\}_{i=1}^{i_{cp,1}-1}$, \dots , $\{D(i)\}_{i=i_{cp,k-1}}^{i_{cp,k}-1}$, \dots , $\{D(i)\}_{i=i_{cp,K-1}}^I$ with $k \in [1, K]$ after $K - 1$ change points have been found.

Let us assume that a reliable PMF estimate of alarm durations can be achieved for the k th segment $\{D(i)\}_{i=i_{cp,k-1}}^{i_{cp,k}-1}$. The corresponding delay timer factor \hat{m}_k for the k th segment can be designed in Eq. (5) via an one-dimensional grid search on m that belongs to the set of positive integers. To deal with the worst scenario, an optimal delay factor is chosen as $\hat{m} = \max(\sum_{k=1}^K \hat{m}_k)$. In practice, a set of delay factors m 's around \hat{m} for different values of $\eta(m)$ in Eq. (4) can be provided as a baseline. Industrial engineers may gain further information from such a baseline, e.g., the sensitivity of \hat{m} with respect to η .

3.3. PMF estimation

The delay factor design relies on a reliable estimate of p_D for a segment $\{D(i)\}_{i=i_{cp,k-1}}^{i_{cp,k}-1}$. The Bayesian estimation approach [33] is exploited to obtain the reliable estimate of p_D as follows. First, let $D_U = \max\{D(i)\}_{i=i_{cp,k-1}}^{i_{cp,k}-1}$ be the upper bound of D , so that the sample space of D is $\{1, 2, \dots, D_U\}$. The sample of D is denoted as d , and $p_D(d)$ is treated as a continuous random variable Θ_d in the range $[0, 1]$,

$$\Theta_d := p_D(d).$$

Without any extra information, it is reasonable to assume that the prior PDF of Θ_d is a continuous uniform distribution,

$$p_{\Theta_d}(\theta_d) = \begin{cases} 1, & 0 < \theta_d < 1 \\ 0, & \text{otherwise} \end{cases}. \quad (9)$$

Let I_D be a discrete random variable taking a sample I_d that is the number of elements in $\{D(i)\}_{i=1}^I$ equal to d , i.e.,

$$I_d = |\{D(i)\}_{i=1}^I = d|. \quad (10)$$

Since each alarm duration is associated with an independent alarm occurrence, I_D follows the binomial distribution with the probability of alarm duration appearances as Θ_d [33],

$$p_{I_D|\Theta_d}(I_d|\Theta_d) = \frac{I!}{I_d!(I-I_d)!} \cdot \Theta_d^{I_d} \cdot (1-\Theta_d)^{I-I_d}. \quad (11)$$

The joint probability distribution of I_D and Θ_d is calculated from Eqs. (9) and (11) via the Bayesian formula as

$$p_{I_D,\Theta_d}(I_d, \Theta_d) = p_{I_d|\Theta_d}(I_d|\Theta_d) \cdot p_{\Theta_d}(\Theta_d).$$

Given the realization I_d in Eq. (10), the posterior probability distribution of Θ_d is

$$p_{\Theta_d|I_D}(\Theta_d|I_d) = \frac{p_{I_D,\Theta_d}(I_d, \Theta_d)}{p_{I_D}(I_d)} = \frac{p_{I_D,\Theta_d}(I_d, \Theta_d)}{\int p_{I_D,\Theta_d}(I_d, \Theta_d) d\Theta_d}. \quad (12)$$

The conditional mean of Θ_d is the Bayesian estimate,

$$\hat{\theta}_d = \int \theta_d \cdot p_{\Theta_d|I_D}(\theta_d|I_d) d\theta_d. \quad (13)$$

Based on Eq. (12), the $(1-\alpha)$ confidence interval of $\hat{\theta}_d$ is obtained as the narrowest interval $[\hat{\theta}_{d,-}, \hat{\theta}_{d,+}]$ satisfying the equality,

$$\int_{\hat{\theta}_{d,-}}^{\hat{\theta}_{d,+}} p_{\Theta_d|I_D}(\theta_d|I_d) d\theta_d = 1 - \alpha. \quad (14)$$

Here α is a small positive number, e.g., $\alpha = 0.05$. Note that $\hat{\theta}_{d,-}$ ($\hat{\theta}_{d,+}$) should be larger (smaller) than 0 (1), since Θ_d is in the range $[0, 1]$.

For each value of d in the sample space $\{1, 2, \dots, D_U\}$, $p_D(d)$ is estimated as $\hat{\theta}_d$ in Eq. (13), i.e.,

$$\hat{p}_D(d) = \hat{\theta}_d. \quad (15)$$

If $\hat{\theta}_d$ is large with respect to the confidence interval $[\hat{\theta}_{d,-}, \hat{\theta}_{d,+}]$ in Eq. (14), e.g.,

$$r(\hat{\theta}_d) := \frac{\hat{\theta}_d}{\max(\hat{\theta}_d - \hat{\theta}_{d,-}, \hat{\theta}_{d,+} - \hat{\theta}_d)} \geq \beta, \quad (16)$$

then $\hat{\theta}_d$ can be regarded as a reliable estimate of $p_D(d)$. A default value of β is set to $\beta = 1$, saying the confidence interval width is no larger than $\hat{\theta}_d$. If the cumulative summation of all reliable estimates $\hat{\theta}_d$'s is larger than a threshold γ , e.g., $\gamma = 90\%$,

$$S_\theta := \sum_{d=1}^{D_U} \hat{\theta}_d \geq \gamma, \text{ for } \hat{\theta}_d \text{ satisfies Eq. (16)}, \quad (17)$$

then it is claimed that \hat{m} in Eq. (5) is designed based on the estimated PMF \hat{p}_D with the certainty level γ . It is generally true that $[\hat{\theta}_{d,-}, \hat{\theta}_{d,+}]$ in Eq. (14) becomes narrower when the number I of alarm duration samples is larger. As an answer to the above critical question, I can be increased gradually till Eq. (17) is satisfied.

3.4. Detailed steps

Based on the above two subsections, the proposed method designs the m -sample delay timer in the following steps:

Step 1: Calculate samples of the alarm duration D in Eq. (6) as $\{D(i)\}_{i=1}^I$ from $\{x_a(t)\}_{t=1}^N$.

Step 2: Detect the distribution change points $\{i_{cp,k}\}_{k=1}^{K-1}$ of $\{D(i)\}_{i=1}^I$, and separate $\{D(i)\}_{i=1}^I$ into K segments as $\{D(i)\}_{i=1}^{i_{cp,1}-1}$, \dots , $\{D(i)\}_{i=i_{cp,k-1}}^{i_{cp,k}-1}$, \dots , $\{D(i)\}_{i=i_{cp,K-1}}^I$ based on these change points.

Step 3: Obtain the reliable PMF estimate in Eq. (15) from each segment $\{D(i)\}_{i=i_{cp,k-1}}^{i_{cp,k}-1}$, and design the proper factor \hat{m}_k in Eq. (5) based on the estimated PMF $\hat{p}_D(d)$.

Step 4: The optimal delay factor is obtained as $\hat{m} = \max(\sum_{k=1}^K \hat{m}_k)$.

Remark 1. This remark revisits the delay timer design method based on the PDF of the process variable x (e.g., that in Taheri-Kalani et al. [28]). If x is IID, then the analytic expression of FAR is available to describe a relationship between m in Eq. (3) and $f(x_a)$ in Eq. (2) [20],

$$f(x_a) = \frac{p_1^m \sum_{i=0}^{m-1} p_2^i}{p_1^m \sum_{i=0}^{m-1} p_2^i + p_2^m \sum_{j=0}^{m-1} p_1^j}, \quad (18)$$

where

$$p_1 = \int_{x_{th}}^{+\infty} p_x(\tilde{x}) d\tilde{x}, \quad p_2 = 1 - p_1. \quad (19)$$

Here p_x is the PDF of x . It is ready to derive the corresponding designing index η as

$$\eta(m) = \frac{O(x_{a,m}(t)_{t=1}^N)}{O(x_a(t)_{t=1}^N)} = \frac{\sum_{i=m}^{\infty} p_2^2 p_1^i}{p_2 p_1}, \quad (20)$$

and the corresponding PMF $p_D(d)$ in Eq. (5) as

$$p_D(d) = p_2 p_1^{d-1}. \quad (21)$$

Given an estimate of p_x , a proper value of m is found as the smallest one satisfying a constraint

$$\sum_{d=\bar{m}}^{+\infty} p_2 p_1^{d-1} \leq \eta_U. \quad (22)$$

However, if x is non-IID, then such an analytic expression is unavailable. In addition, since the PDF of x is required, the design of m in Eq. (22) is limited to analog process variables only.

Remark 2. This remark discusses the relationship between m and EDD. If x is IID and changes suddenly from normal to abnormal conditions, EDD can be obtained as [20]

$$\text{EDD}(m) = \frac{1 - p_1^m - p_2 p_1^m}{p_2 p_1^m}, \quad (23)$$

where p_1 and p_2 are given in Eq. (19). Clearly, $\text{EDD}(m)$ increases with the increment of m . If x is non-IID and changes gradually from normal to abnormal conditions, $\text{EDD}(m)$ depends on the changing states between normal and abnormal conditions of x . An analytic expression of $\text{EDD}(m)$ is not available in the literature. Even so, it is evident that $\text{EDD}(m)$ increases with the increment of m . Thus, the smallest one satisfying Eq. (5) is selected as the proper value \hat{m} to make $\text{EDD}(m)$ as small as possible.

4. Examples

This section presents four examples to illustrate the proposed method. The data and Matlab programs are accessible at: <https://ieee-datalog.org/documents/dataset-delay-timer-design>.

Example 1. An example based on the continuous stirred tank reactor (CSTR) is adopted to validate the proposed method. The CSTR model is often used as a well-established benchmark for process control and monitoring [34].

As shown in Fig. 2, a reactant A (cyclopentadiene) is fed in the CSTR with initial concentration C_{A0} , flow q , and temperature

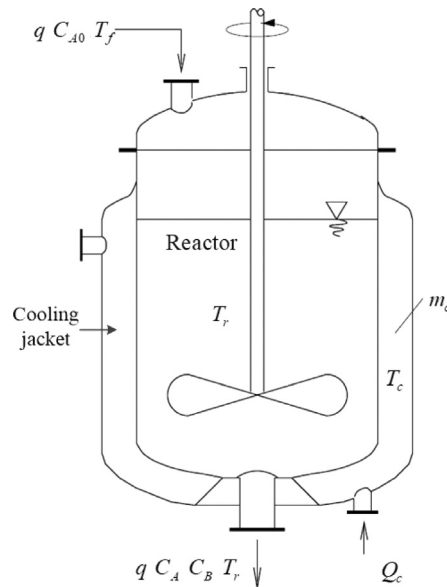


Fig. 2. The CSTR with a cooling jacket in Example 1.

T_f . Three reactions may occur in the reactor as a main reaction $A \rightarrow B$, a follow-up reaction $B \rightarrow C$, and a side reaction $2A \rightarrow E$ [35]:



Here, B (cyclopentene) is the desired product, C (cyclopentanone) and E (dicyclopentadiene) are undesirable byproducts, and k_i 's are the reaction velocities. The dynamic model of CSTR is obtained based on the material balance of concentrations C_A for the reactant A and C_B for the desired product B , as well as the energy balance for the reactor and the cooling jacket with temperatures T_r and T_c [35]:

$$\begin{aligned} \frac{dC_A(t)}{dt} &= \frac{q}{V} (C_{A0} - C_A(t)) - k_1(T_r(t))C_A(t) - k_3(T_r(t))C_A^2(t), \\ \frac{dC_B(t)}{dt} &= -\frac{q}{V} C_B(t) + k_1(T_r(t))C_A(t) - k_2(T_r(t))C_B(t), \\ \frac{dT_r(t)}{dt} &= \frac{q}{V} (T_f - T_r(t)) - \frac{1}{\rho C_p} (k_1(T_r(t))C_A(t)\Delta H_{AB} \\ &\quad + k_2(T_r(t))C_B(t)\Delta H_{BC} + k_3(T_r(t))C_A^2(t)\Delta H_{AD}) \\ &\quad + \frac{k_w A_R}{V \rho C_p} (T_c(t) - T_r(t)), \\ \frac{dT_c(t)}{dt} &= \frac{1}{m_c C_{pc}} (-Q_c + k_w A_R (T_r(t) - T_c(t))). \end{aligned} \quad (25)$$

Here t is the sampling index, and the reaction velocities $k_i(T_r(t))$ are obtained via Arrhenius functions of the temperature (in °C):

$$k_i(T_r(t)) = k_{i0} e^{-\frac{E_i}{(T_r(t)+273.15)}}, \quad i = 1, 2, 3. \quad (26)$$

The CSTR model in this example contains four input variables as C_{A0} , T_f , q , and Q_c and four output variables as C_A , C_B , T_r , and T_c . Here, Q_c is the heat removal generated in the chemical reactions by coolants in the cooling jacket. The model parameters in Eqs. (25) and (26) are listed in Table 1. The CSTR is assumed to be initialized at an operating point with input variables as $C_{A0} = 5.1 \frac{\text{mol}}{\text{l}}$, $q = 141.9 \frac{\text{l}}{\text{h}}$, $T_f = 104.9^\circ\text{C}$, and $Q_c = 1113.5 \frac{\text{kJ}}{\text{h}}$. Table 2 shows the corresponding low-alarm thresholds, which

Table 1
The CSTR model parameters.

| Model parameter | Symbol | Value | Unit |
|--|-----------------|-----------------------|--|
| Collision factor for reaction k_1 | k_{10} | $1.287 \cdot 10^{12}$ | $\frac{1}{\text{h}}$ |
| Collision factor for reaction k_2 | k_{20} | $1.287 \cdot 10^{12}$ | $\frac{1}{\text{h}}$ |
| Collision factor for reaction k_3 | k_{30} | $9.043 \cdot 10^9$ | $\frac{1}{\text{mol} \cdot \text{h}}$ |
| Activation energy for reaction k_1 | E_1 | 9758.3 | K |
| Activation energy for reaction k_2 | E_2 | 9758.3 | K |
| Activation energy for reaction k_3 | E_3 | 8560 | K |
| Enthalpy of reaction k_1 | ΔH_{AB} | 4.2 | $\frac{\text{kJ}}{\text{mol}}$ |
| Enthalpy of reaction k_2 | ΔH_{BC} | -11.0 | $\frac{\text{kJ}}{\text{mol}}$ |
| Enthalpy of reaction k_3 | ΔH_{AD} | -41.85 | $\frac{\text{kJ}}{\text{mol}}$ |
| Density of reactant | ρ | 0.9342 | $\frac{1}{\text{kg}}$ |
| Reactant heat capacity | C_p | 3.01 | $\frac{\text{kJ}}{\text{kg} \cdot \text{K}}$ |
| Coolant heat capacity | C_{pc} | 2.0 | $\frac{\text{kJ}}{\text{kg} \cdot \text{K}}$ |
| Cooling jacket heat transfer coefficient | k_w | 4032 | $\frac{\text{W}}{\text{m} \cdot \text{K}}$ |
| Cooling jacket surface | A_R | 0.215 | m^2 |
| Reactor volume | V | 0.01 | m^3 |
| Coolant mass | m_c | 5.0 | kg |

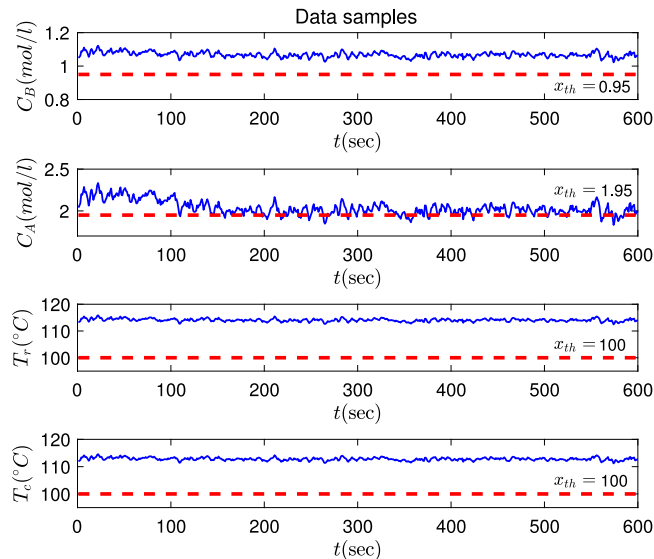


Fig. 3. Data samples of four output variables (blue solid) with low-alarm thresholds (red dash) in Example 1.

Table 2
Low-alarm thresholds of four output variables.

| Process variable | Threshold | Unit |
|------------------|-----------------|-------------------------------|
| C_B | $x_{th} = 1.95$ | $\frac{\text{mol}}{\text{l}}$ |
| C_A | $x_{th} = 0.95$ | $\frac{\text{mol}}{\text{l}}$ |
| T_r | $x_{th} = 100$ | °C |
| T_c | $x_{th} = 100$ | °C |

Table 3
Delay factors \hat{m} 's and corresponding values of η in Example 1.

| \hat{m} | η | \hat{m} | η |
|-----------|--------|-----------|--------|
| 9 | 0.0223 | 6 | 0.0659 |
| 8 | 0.0329 | 5 | 0.0766 |
| 7 | 0.0552 | 4 | 0.1322 |

are set according to the variation ranges suggested in Chen et al. [35].

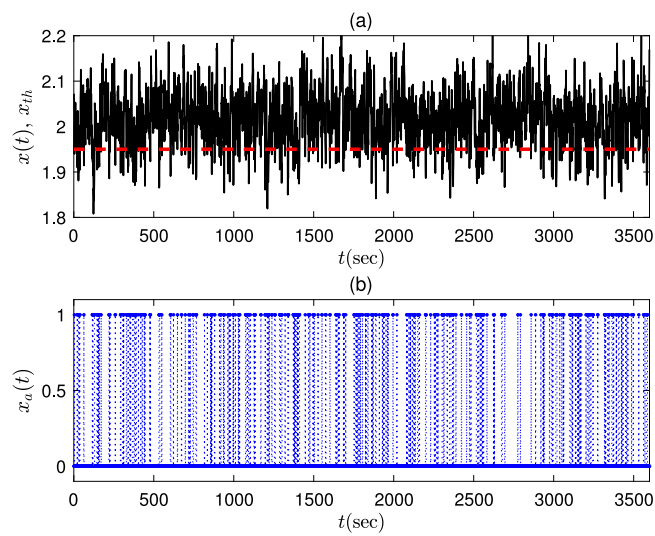


Fig. 4. (a) One-hour samples of x (black solid) and its high-alarm threshold x_{th} (red dash). (b) Corresponding samples of x_a in Example 1.

Data samples of four output variables are shown in Fig. 3 with sampling period 1 s. Each output variable is contaminated by colored noise $v(t) = 0.8v(t-1) - 0.1v(t-2) + e(t)$, where $e(t)$ is Gaussian white noise with zero mean and variance σ_e^2 . Realizations of the white noise $e(t)$ for four output variables are mutually independent, with $\sigma_e^2 = 0.04$ for C_A , $\sigma_e^2 = 0.01$ for C_B , $\sigma_e^2 = 0.36$ for T_r and T_c . The working condition changes at $t = 100$ in Fig. 3 with q changing from $141.9 \frac{1}{\text{h}}$ to $120 \frac{1}{\text{h}}$. Four output variables are still in the normal condition as noise free data samples are higher than the low-alarm threshold, but false alarms occur in C_A due to the colored noise $v(t)$, as shown in Fig. 3.

Data samples of C_A with false alarms are considered as x to design m -delay timer in this example. Clearly, x is non-IID with colored noise $v(t)$. For illustration, one-hour data samples of x are shown in Fig. 4-(a). The proposed method is applied to design the m -sample delay timer. No change points are found in the alarm durations of this one-hour data samples from Eqs. (7) and (8). 50 alarm durations are sufficient to obtain a reliable estimate of the alarm duration PMF as S_θ in Eq. (17) becomes larger than $\gamma = 0.9$ after $I = 50$ in Fig. 5-(a). The Bayesian estimates of $\hat{\theta}_d$ in Eq. (13) for $d = 1, 2, \dots, 9$ together with their 95% confidence intervals of $[\hat{\theta}_{d,-}, \hat{\theta}_{d,+}]$ in Eq. (14) are given in Fig. 5-(b). Based on the reliable estimate of PMF, $\hat{m} = 8$ in Eq. (5) is obtained by using the upper bound $\eta_U = 0.05$. Table 3 lists delay factors \hat{m} 's and corresponding values of η as a baseline.

The delay timer with $\hat{m} = 8$ is applied to the next-hour samples of x_a . As a result, $x_{a,\hat{m}}$ in Fig. 6-(c) has 6 alarm occurrences, while x_a in Fig. 6-(b) suffers from 250 false alarms, i.e., 97.6% false alarms in x_a are removed in $x_{a,\hat{m}}$ as designed. The FAR in Eq. (2) is $f(x_{a,\hat{m}}) = 0.0361$ for $\hat{m} = 8$.

As a comparison, the existing method based on the PDF of x (e.g., that in Taheri-Kalani et al. [28]) is applied here. The estimated PDF of x based on data samples of $x(t)$ in Fig. 4-(a) is shown in Fig. 5-(c) with $p_1 = 0.1472$ in Eq. (19). The delay factor is designed by Eq. (22) as $\tilde{m} = 3$ with designing index $\eta(\tilde{m})$ in Eq. (20) no larger than 0.05. The delay timer with $\tilde{m} = 3$ is applied to the next-hour samples of x_a in Fig. 6; as a result, $x_{a,\tilde{m}}$ in Fig. 6-(d) has 85 alarm occurrences while $x_{a,\hat{m}}$ in Fig. 6-(c) has 6 alarm occurrences. The FAR in Eq. (2) is calculated for $x_{a,\hat{m}}$ as $f(x_{a,\hat{m}}) = 0.1236$, much larger than the counterpart $f(x_{a,\tilde{m}}) = 0.0361$ from

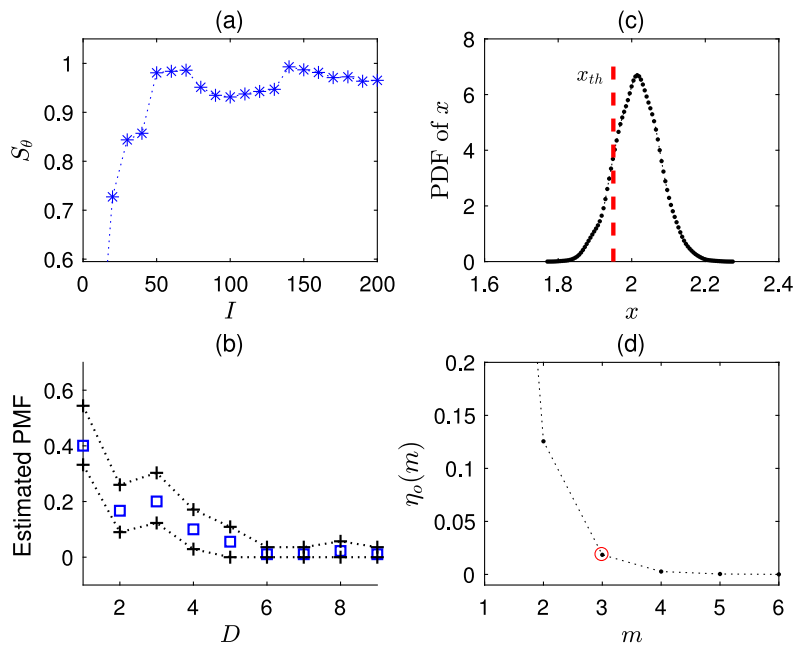


Fig. 5. (a) S_θ as a function of I , (b) $\hat{\theta}_d$ (blue square) and $[\hat{\theta}_{d,-}, \hat{\theta}_{d,+}]$ (black cross) for $I = 50$, (c) p_x (black dot) and x_{th} (red dash), (d) $\eta(m)$ in Example 1.

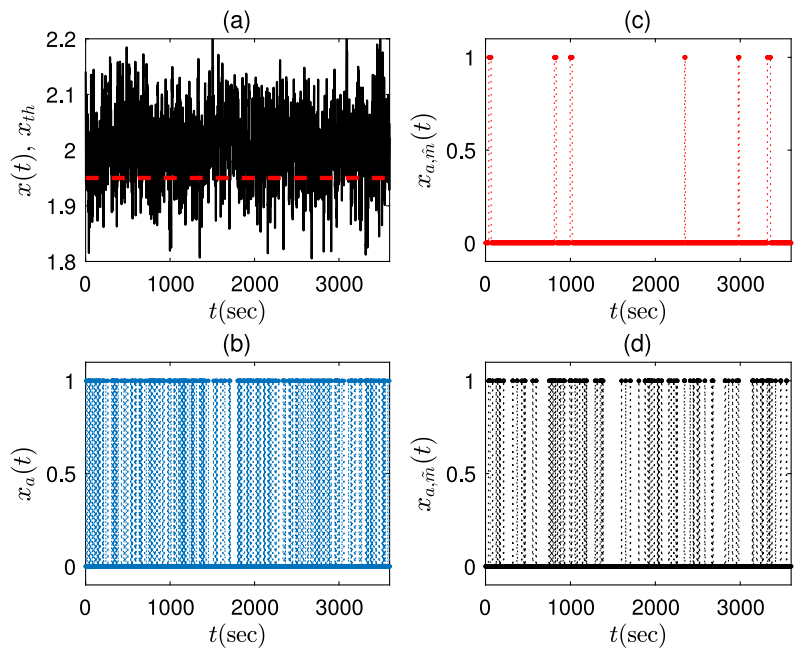


Fig. 6. (a) Next one-hour samples of x (black solid) and x_{th} (red dash), (b) x_a , (c) $x_{a,\hat{m}}$, (d) $x_{a,\tilde{m}}$ in Example 1.

the proposed method. The failure of the existing method is due to a fact that x is non-IID with the colored noise $v(t)$.

Example 2. This example is used to illustrate Steps 2 and 3 of the proposed method, namely, the distribution change detection for D and the Bayesian estimation for the PMF of D . Consider a discrete random variable D representing the alarm duration with a theoretical PMF as

$$p_D(d) = \begin{cases} 0.1, & \text{if } d = 2, \\ 0.2, & \text{if } d = 3, \\ 0.4, & \text{if } d = 4, \\ 0.25, & \text{if } d = 5, \\ 0.05, & \text{if } d = 6. \end{cases} \quad (27)$$

The PMF p_D is estimated by Step 2 of the proposed method. A set of sequences $\{D(i)\}_{i=1}^I$ for $I = 50$ is generated, where I_d in Eq. (10) takes the values 8, 10, 20, 11, 1 for $d = 2, 3, \dots, 6$, respectively. Fig. 7-(a) presents the five estimated posterior PDFs of $p_{\Theta_d|D}$ in Eq. (12) for $d = 2, 3, \dots, 6$. Fig. 7-(b) gives the Bayesian estimates of $\hat{\theta}_d$ in Eq. (13) for $d = 2, 3, \dots, 6$ together with their 95% confidence intervals. Table 4 lists the concrete values of $\hat{\theta}_d$, $[\hat{\theta}_{d,-}, \hat{\theta}_{d,+}]$ in Eq. (14) and $r(\hat{\theta}_d)$ in Eq. (16). The calculations are repeated for 100 Monte Carlo simulations. As shown in Fig. 8, the numbers of simulations that an actual PMF value θ_d lies inside its 95% confidence interval $[\hat{\theta}_{d,-}, \hat{\theta}_{d,+}]$ are respectively equal to 95, 94, 96, 97, 100 for $d = 2, 3, \dots, 6$. The

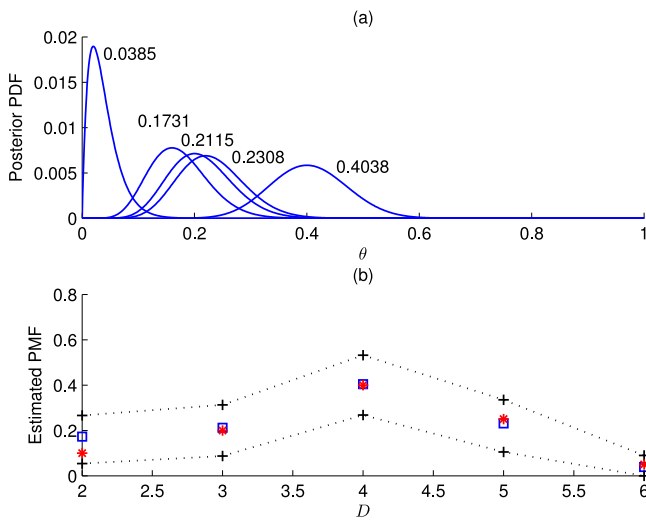


Fig. 7. (a) Estimated posterior PDFs of $p_{\theta_d|l_D}$, (b) Bayesian estimates (blue square) of $\hat{\theta}_d$ together with their confidence intervals (black cross) of $[\hat{\theta}_{d,-}, \hat{\theta}_{d,+}]$, and actual PMF values (red stars) for $d = 2, 3, \dots, 6$ in Example 2.

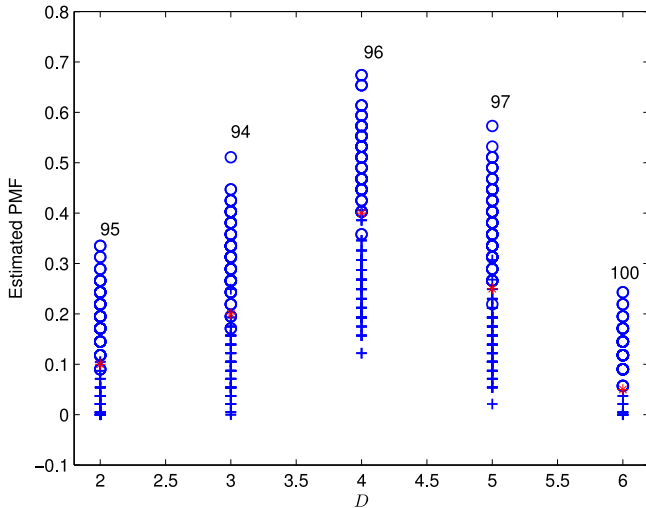


Fig. 8. Upper (blue circle) and lower (blue cross) bounds of confidence intervals of Bayesian estimates in 100 Monte Carlo simulations and actual PMF values (red star) in Example 2.

Table 4
Estimated PMFs and their confidence intervals in Example 2.

| d | $\hat{\theta}_d$ | $[\hat{\theta}_{d,-}, \hat{\theta}_{d,+}]$ | $r(\hat{\theta}_d)$ |
|-----|------------------|--|---------------------|
| 2 | 0.1731 | [0.0540, 0.2660] | 1.4535 |
| 3 | 0.2115 | [0.0870, 0.3130] | 1.6986 |
| 4 | 0.4038 | [0.2680, 0.5320] | 2.9728 |
| 5 | 0.2308 | [0.1050, 0.3350] | 1.8349 |
| 6 | 0.0385 | [0.0000, 0.0900] | 0.7465 |

above results clearly support the validness of Bayesian estimates and their confidence intervals.

The validness of the distribution change detection is verified as follows. Consider an alarm duration samples $\{D(i)\}_{i=1}^{300}$. The first 100 samples $\{D(i)\}_{i=1}^{100}$ are generated by Eq. (27), the second 100 samples $\{D(i)\}_{i=101}^{200}$ are generated by Eq. (28), and the last 100 samples $\{D(i)\}_{i=201}^{300}$ are generated by Eq. (27). Obviously, the distribution changes at $t = 100$ and $t = 200$. $U_{i,l}$ in Eq. (7) is

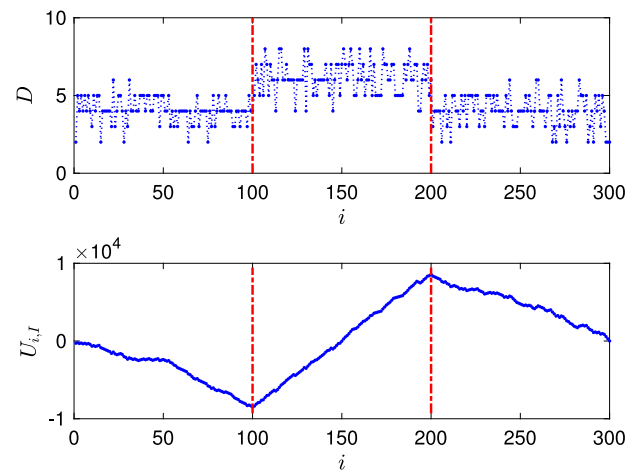


Fig. 9. (a) Data samples (blue dash-dotted) and change points (red dash), (b) $U_{i,l}$ (blue solid) and change points (red dash) of $\{D(i)\}_{i=1}^{300}$ in Example 2.

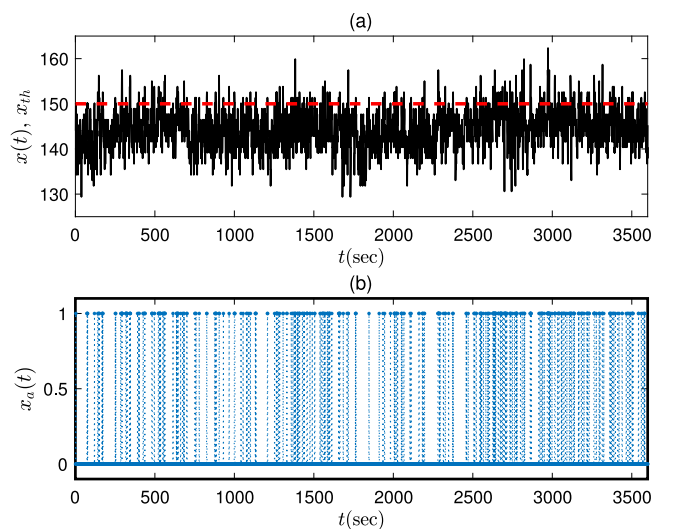


Fig. 10. (a) One-hour samples of x (black solid) and its high-alarm threshold x_{th} (red dash), (b) Corresponding samples of x_a in Example 3.

shown in Fig. 9-(b) with two evident maximum and minimum values. Thus, two change points are found as $i_{cp,1} = 100$ and $i_{cp,2} = 200$, which are consistent with the actual distribution changes.

$$p_D(d) = \begin{cases} 0.05, & \text{if } d = 4, \\ 0.25, & \text{if } d = 5, \\ 0.4, & \text{if } d = 6, \\ 0.2, & \text{if } d = 7, \\ 0.1, & \text{if } d = 8. \end{cases} \quad (28)$$

Example 3. This is an industrial example to confirm the useability of the proposed method in the real industrial process. An industrial process variable x with tagname X71NAO067 is the pressure difference between the upper and middle catalyst layers in a furnace reaction zone of a thermal power plant. It is configured with a high-alarm threshold $x_{th} = 150$ Pa. Fig. 10-(a) shows one-hour data samples of x with a sampling period 1 s. Obviously, the averaged level of $\{x(t)\}_{t=1}^{3600}$ is smaller than x_{th} , and x is in the normal condition. However, x is contaminated by severe noises so that it suffers from a large amount of false alarms in Fig. 10-(b).

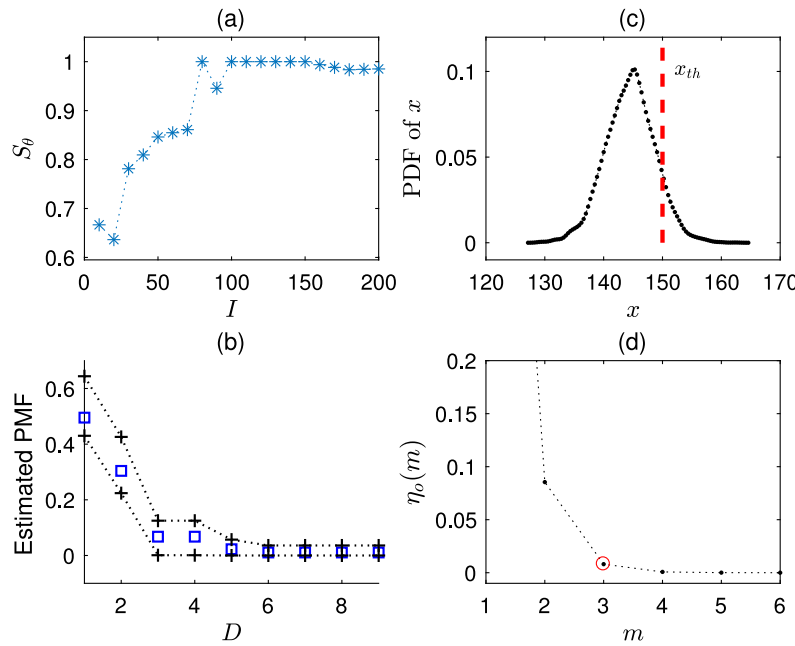


Fig. 11. (a) S_θ as a function of I , (b) $\hat{\theta}_d$ (blue square) and $[\hat{\theta}_{d,-}, \hat{\theta}_{d,+}]$ (black cross) for $I = 80$, (c) p_x (black dot) and x_{th} (red dash), (d) $\eta_0(m)$ in Example 3.

Table 5

Delay factors \hat{m} 's and corresponding values of η in Example 3.

| \hat{m} | η | \hat{m} | η |
|-----------|--------|-----------|--------|
| 7 | 0.0216 | 4 | 0.0657 |
| 6 | 0.0324 | 3 | 0.1333 |
| 5 | 0.0432 | 2 | 0.2008 |

The proposed method is applied to design the m -sample delay timer. No change points are found from Eqs. (7) and (8) in the alarm durations of this one-hour data samples. Fig. 11-(a) presents S_θ in Eq. (17) as a function of the sample size I of alarm durations. It is observed that S_θ becomes larger than $\gamma = 0.9$ after $I = 80$. In words, 80 alarm durations are sufficient to obtain a reliable estimate of the alarm duration PMF. Fig. 11-(b) gives the Bayesian estimates of $\hat{\theta}_d$ in Eq. (13) for $d = 1, 2, \dots, 9$ together with their 95% confidence intervals of $[\hat{\theta}_{d,-}, \hat{\theta}_{d,+}]$ in Eq. (14), from which $\hat{m} = 5$ in Eq. (5) is obtained by using the upper bound $\eta_U = 0.05$. Table 5 gives the delay factors \hat{m} 's and corresponding values of η as a baseline.

The delay timer with $\hat{m} = 5$ is applied to the next-hour samples of x_a , where x is in the normal condition as shown in Fig. 12. As a result, $x_{a,\hat{m}}$ in Fig. 12-(c) has 14 alarm occurrences, while x_a in Fig. 12-(b) suffers from 294 false alarms, i.e., 95.24% false alarms in x_a are removed in $x_{a,\hat{m}}$ as designed. The FAR in Eq. (2) is $f(x_{a,\hat{m}}) = 0.0325$ for $\hat{m} = 5$.

As a comparison, the existing method based on the probability distribution of x (e.g., Taheri-Kalani et al. [28]) is applied here. Fig. 11-(c) shows the estimated PDF of x based on data samples of $x(t)$ in Fig. 10-(a), from which $p_1 = 0.0944$ in Eq. (19) and $\tilde{m} = 3$ in Eq. (22) are obtained to make the designing index $\eta(\tilde{m})$ in Eq. (20) no larger than 0.05. The delay timer with $\tilde{m} = 3$ is applied to the next-hour samples of x_a in Fig. 12; as a result, $x_{a,\tilde{m}}$ in Fig. 12-(d) has 78 alarm occurrences larger than 14 alarm occurrences in the proposed method. The FAR in Eq. (2) is calculated for $x_{a,\tilde{m}}$ as $f(x_{a,\tilde{m}}) = 0.0961$, larger than the counterpart $f(x_{a,\hat{m}}) = 0.0325$ from the proposed method.

Table 6

Delay factors \hat{m} 's and corresponding values of η in Example 4.

| \hat{m} | η | \hat{m} | η |
|-----------|--------|-----------|--------|
| 86 | 0.0739 | 91 | 0.0451 |
| 87 | 0.0649 | 92 | 0.0424 |
| 88 | 0.0578 | 93 | 0.0405 |
| 89 | 0.0515 | 94 | 0.0378 |
| 90 | 0.0471 | 95 | 0.0359 |

Example 4. The proposed method is applied to a digital process variable in this example. A digital process variable 4U30LS53 is used to indicate an abnormality that the water level inside a low-pressure heater is below a certain level at a thermal power plant. The alarm threshold x_{th} in Eq. (1) is equal to 1, so that x and x_a are the same. Fig. 13 presents four-hour data samples of x with a sampling period 1 s. Occasionally, x_a runs into the alarm state. However, all these alarms are false ones: a feedback controller is operating in a real time to maintain the water level at a desired level; when a disturbance comes, it takes a while for the water level returning to the desired value. As a result, industrial plant operators do not need to take any corrective actions when alarms like those in Fig. 13 appear and disappear in an automatic manner. Along with the digital process variable 4U30LS53, an analog process variable 4U30LT58 is the measurement of the water level inside a low-pressure heater, and is configured with a low alarm threshold $x_{th} = -50$. In other words, the water level is simultaneously monitored by two independent digital and analog sensors. However, as shown in Figs. 13 and 14, the analog process variable is always in the normal condition with no alarms, while the digital process variable has many nuisance alarms. Thus, it is necessary to design the delay timer for the digital process variable to reduce the influence of nuisance alarms.

The proposed method is applied to design the m -sample delay timer for x_a . Note that most of contemporary methods need probability density functions of analog process variables, so that they cannot be applied here. Fig. 15-(a) presents alarm durations

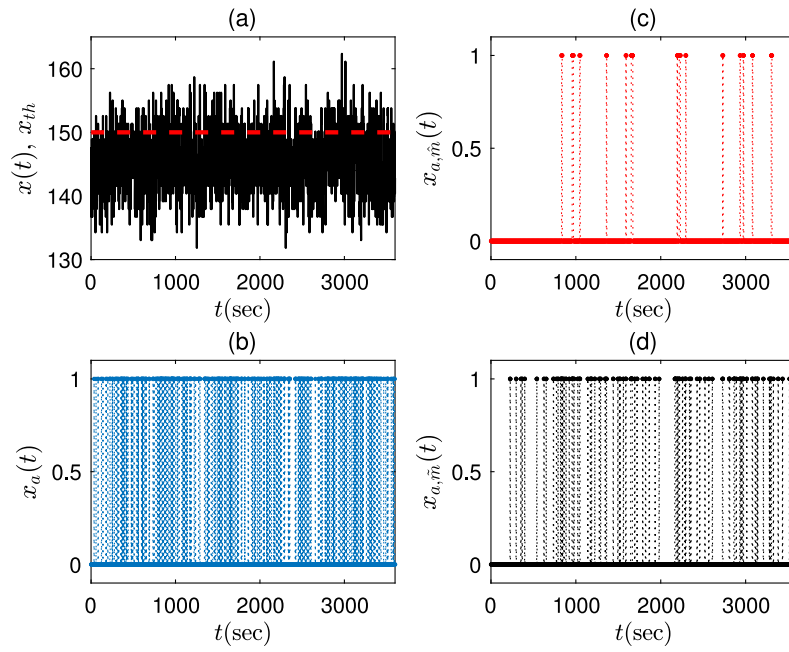


Fig. 12. (a) Next one-hour samples of x (black solid) and x_{th} (red dash), (b) x_a , (c) $x_{a,\hat{m}}$, (d) $x_{a,\tilde{m}}$ in Example 3.

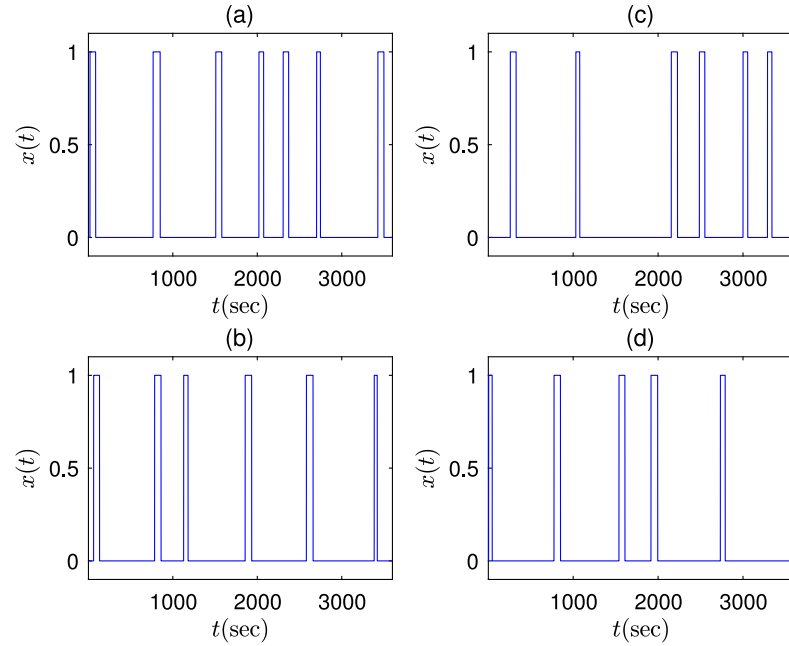


Fig. 13. Four-hour data samples of x in Example 4.

of x_a in 20 days, and Fig. 15-(b) shows S_θ in Eq. (17) as a function of I . Two estimated PMFs of alarm durations for $I = 100$ and $I = 1000$ are respectively given in Figs. 15-(c) and (d). The confidence intervals in Fig. 15-(c) are quite wide, so that the estimated PMF therein is not reliable. If the estimated PMF in Fig. 15-(c) is used, then the delay factor becomes $\hat{m} = 137$, which is too large as revealed from samples of alarm durations in Fig. 15-(a). The above results demonstrate the necessity of having a reliable PMF estimation. In contrast, the estimated PMF in Fig. 15-(d) is reliable, for being associated with S_θ close to 1 and relatively narrow confidence intervals therein. The optimal value $\hat{m} = 90$ is obtained by using $\eta_U = 0.05$ based on the

estimated PMF in Fig. 15-(d). Delay factors \hat{m} 's and corresponding values of η are shown in Table 6 as a baseline. The variable 4U30LS53 in this example is used to monitor the water level, and the recommendation of delay factor m for the water level in an industrial standard EEMUA [2] is 60 s. As shown in Fig. 14, the corresponding water level with the sampling period 1 s changes slowly. Thus, $\hat{m} = 90$ is a reasonable choice for this variable.

The delay timer with $\hat{m} = 90$ is applied to another 10 days samples of x_a . With delay timer designed, about 97.4% false alarms in x_a are removed in $x_{a,\hat{m}}$ as 14 alarm occurrences in $x_{a,\hat{m}}$ and 556 false alarms in x_a . The FAR in Eq. (2) is $f(x_{a,\hat{m}}) = 0.025$ for $\hat{m} = 90$.

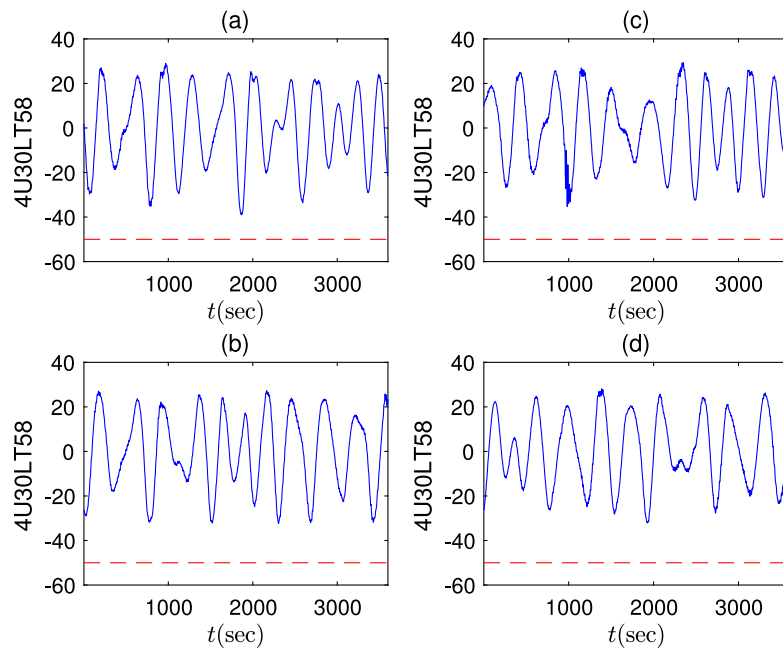


Fig. 14. Four-hour data samples of 4U30LT58 (blue solid) and its low-alarm threshold (red dash) in Example 4.

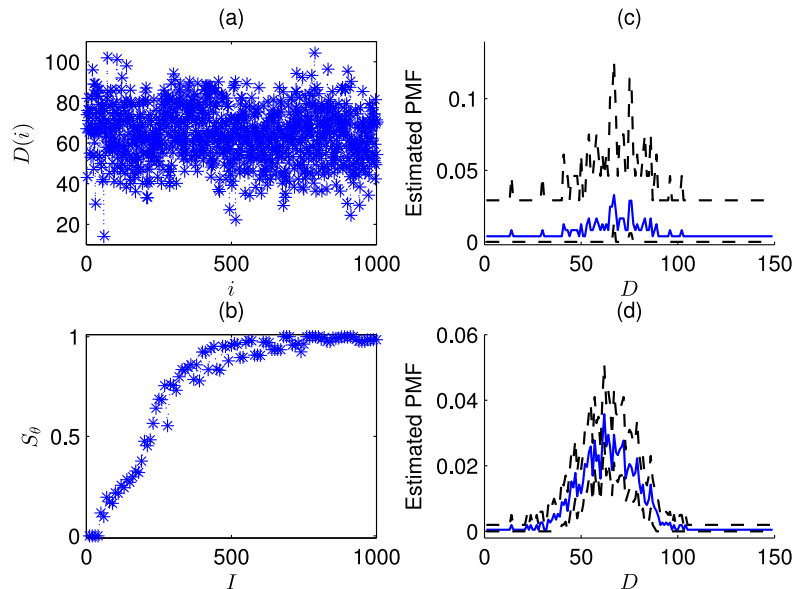


Fig. 15. (a) Alarm durations, (b) S_θ as a function of I , (c) $\hat{\theta}_d$ (blue square) and $[\hat{\theta}_{d,-}, \hat{\theta}_{d,+}]$ (black cross) for $I = 100$, (d) the counterparts of (c) for $I = 1000$ in Example 4.

5. Conclusion

This paper proposed a new method to design the m -sample delay timer for removing false alarms when a process variable was operating in the normal condition. By noticing that nuisance alarms with durations less than m samples are removed by the m -sample delay timer, the delay factor m was designed based on the PMF of alarm durations. Two technical challenges were resolved by the distribution change detection for ensuring segments of alarm durations with same distributions, and the Bayesian estimation for obtaining reliable PMF estimates for alarm durations. Contemporary methods were based on the PDFs of process variables, so that they were confined to analog process variables that were required to be IID. In contrast, the proposed method

extended the applicability scope for being applicable to both analog and digital process variables without the IID requirement. Numerical and industrial examples illustrated the effectiveness of the proposed method.

CRediT authorship contribution statement

Jiandong Wang: Conceptualization, Methodology, Software, Writing – original draft, Writing – review & editing, Supervision, Funding acquisition. **Zhen Wang:** Methodology, Software, Investigation, Data curation, Writing (revision), Visualization. **Xuan Zhou:** Methodology, Software, Investigation, Data curation, Writing – original draft, Visualization. **Fan Yang:** Conceptualization, Validation, Writing – review & editing.

Declaration of competing interest

The authors declare that they have no known competing financial interests or personal relationships that could have appeared to influence the work reported in this paper.

References

- [1] ISA, ISA-18.2: Management of Alarm Systems for the Process Industries, International Society of Automation, 2009.
- [2] EEMUA, EEMUA-191: Alarm Systems – a Guide To Design, Management and Procurement, Engineering Equipment and Materials Users Association, 2013.
- [3] J. Wang, F. Yang, T. Chen, S.L. Shah, An overview of industrial alarm systems: Main causes for alarm overloading, research status, and open problems, *IEEE Trans. Autom. Sci. Eng.* 13 (2016) 1045–1061.
- [4] P. Goel, A. Datta, M.S. Mannan, Industrial alarm systems: Challenges and opportunities, *J. Loss Prev. Process Ind.* 50 (2017) 23–36.
- [5] M.L. Bransby, J. Jenkinson, The management of alarm systems, in: Health and Safety Executive, 1998.
- [6] D. Rothenberg, *Alarm Management for Process Control*, Momentum Press, 2009.
- [7] V.B. Soares, J.C. Pinto, M.B. Souza de, Alarm management practices in natural gas processing plants, *Control Eng. Pract.* 55 (2016) 185–196.
- [8] W. Hu, T. Chen, S.L. Shah, Discovering association rules of mode-dependent alarms from alarm and event logs, *IEEE Trans. Control Syst. Technol.* 26 (2017) 971–983.
- [9] Y. Yu, J. Wang, Alarm monitoring for multivariate processes based on a convex-hull normal operating zone, *IEEE Trans. Control Syst. Technol.* 28 (2020) 2649–2656.
- [10] W. Hu, T. Chen, S.L. Shah, Detection of frequent alarm patterns in industrial alarm floods using itemset mining methods, *IEEE Trans. Ind. Electron.* 65 (2018) 7290–7300.
- [11] C. Tian, C. Zhao, Single model-based analysis of relative causal changes for root-cause diagnosis in complex industrial processes, *Process Safety Environ. Protect.* 60 (2021) 12602–12613.
- [12] Y. Xu, J. Wang, Y. Yu, Alarm event prediction from historical alarm flood sequences based on Bayesian estimators, *IEEE Trans. Autom. Sci. Eng.* 17 (2020) 1070–1075.
- [13] Y. Zhang, H. Fang, Y. Zheng, X. Li, Torus-event-based fault diagnosis for stochastic multirate time-varying systems with constrained fault, *IEEE Trans. Cybern.* 50 (2020) 2803–2813.
- [14] M.S. Rahman, F. Khan, A. Shaikh, S. Ahmed, A conditional dependence-based marine logistics support risk model, *Reliab. Eng. Syst. Saf.* 193 (2020) 106623.
- [15] M.T. Amin, F. Khan, S. Ahmed, S. Imtiaz, Risk-based fault detection and diagnosis for nonlinear and non-Gaussian process systems using R-vine copula, *Process Safety Environ. Protect.* 150 (2021) 123–136.
- [16] R. Arunthanathan, F. Khan, S. Ahmed, S. Imtiaz, A deep learning model for process fault prognosis, *Process Safety Environ. Protect.* 154 (2021) 467–479.
- [17] B. Hollifield, E. Habibi, *The Alarm Management Handbook*, second ed., PAS, 2010.
- [18] N.A. Adnan, I. Izadi, T. Chen, On expected detection delays for alarm systems with deadbands and delay-timers, *J. Process Control* 21 (2011) 1318–1331.
- [19] E. Naghossi, I. Izadi, T. Chen, Estimation of alarm chattering, *IEEE Trans. Autom. Sci. Eng.* 9 (2011) 296–307.
- [20] J. Xu, J. Wang, I. Izadi, T. Chen, Performance assessment and design for univariate alarm systems based on FAR, MAR, and AAD, *IEEE Trans. Autom. Sci. Eng.* 9 (2012) 296–307.
- [21] N.A. Adnan, Y. Cheng, I. Izadi, T. Chen, Study of generalized delay-timers in alarm configuration, *J. Process Control* 23 (2013) 382–395.
- [22] J. Wang, T. Chen, An online method to remove chattering and repeating alarms based on alarm durations and intervals, *Comput. Chem. Eng.* 67 (2014) 43–52.
- [23] M.S. Afzal, M. Shahzad, T. Chen, Analysis and design of multimode delay-timers, *Chem. Eng. Res. Des.* 120 (2017) 179–193.
- [24] Z. Zeng, W. Tan, R. Zhou, Performance assessment for generalized delay-timers in alarm configuration, *J. Process Control* 57 (2014) 80–101.
- [25] A. Tulsky, F. Alrowaie, B. Gopaluni, Design and assessment of delay timer alarm systems for nonlinear chemical processes, *AIChE J.* 64 (2018) 77–90.
- [26] M.S. Afzal, T. Chen, Analysis and design of time-deadbands for univariate alarm systems, *Control Eng. Pract.* 71 (2018) 96–107.
- [27] J. Su, C. Guo, H. Zang, F. Yang, D. Huang, X. Gao, Y. Zhao, A multi-setpoint delay-timer alarming strategy for industrial alarm monitoring, *J. Loss Prev. Process Ind.* 54 (2018) 1–9.
- [28] J. Taheri-Kalani, G. Latif-Shabgahi, M. Alyari Shoorehdeli, On the use of penalty approach for design and analysis of univariate alarm systems, *J. Process Control* 69 (2018) 103–113.
- [29] R. Kaced, A. Kouadri, K. Baiche, Designing alarm system using modified generalized delay-timer, *J. Loss Prev. Process Ind.* 61 (2019) 40–48.
- [30] Z. Wang, X. Bai, J. Wang, Z. Yang, Indexing and designing deadbands for industrial alarm signals, *IEEE Trans. Ind. Electron.* 66 (2019) 8093–8103.
- [31] J. Wang, Z. Yang, K. Chen, D. Zhou, Practices of detecting and removing nuisance alarms for alarm overloading in thermal power plants, *Control Eng. Pract.* 67 (2017) 21–30.
- [32] A.N. Pettit, A non-parametric approach to the change-point problem, *Appl. Stat.* 28 (1979) 126–135.
- [33] R.E. Walpole, R.H. Myers, S.L. Myers, K. Ye, *Probability and Statistics for Engineers and Scientists*, ninth ed., Prentice Hall, 2011.
- [34] A. Kroll, H. Schulte, Benchmark problems for nonlinear system identification and control using soft computing methods: Need and overview, *Appl. Soft Comput.* 25 (2014) 496–513.
- [35] H. Chen, A. Kremling, F. Allgower, Nonlinear predictive control of a benchmark CSTR, in: Proceedings of 3rd European control conference, 1995, pp. 3247–3252.